



Energy Management Strategy for Grid-Tied Photovoltaic Systems with Integrated Hybrid Energy Storage

Thadapakelli Lavanya¹, Bachu Asreetha², Bogimi Sirisha³.

1. Department of Electrical Engineering - College of Engineering – Osmania University, Hyderabad - Telangana
lavanya.t253@gmail.com
2. Department of Electrical Engineering - College of Engineering – Osmania University, Hyderabad - Telangana
asreetha123@gmail.com
3. Associate Professor-Department of Electrical Engineering - College of Engineering – Osmania University, Hyderabad – Telangana
sirishab2007@gmail.com

Correspondence:

Bogimi Sirisha

Associate Professor-Department of Electrical Engineering -University College of Engineering – Osmania University, Hyderabad – Telangana Email:

sirishab2007@gmail.com

Abstract

Micro grids play a crucial role in facilitating the integration of renewable energy sources at the local level, fostering energy resilience and sustainability. Integrating RES, such as photovoltaic (PV) systems, can indeed introduce fluctuations and instability into the grid due to its intermittent nature. This paper presents an efficient energy management scheme for integrating renewable energy sources (RES) into the power grid, utilizing a hybrid configuration of battery and supercapacitor storage systems. By regulating the allocation of power among the battery, supercapacitor, and the utility grid according to the charging levels (SOC), a practical approach is provided to optimize the system's performance. This not only helps in mitigating PV power fluctuations but also ensures that the battery undergoes less strain by leveraging the supercapacitor to manage abrupt changes in power generation or load demand. The effectiveness of proposed energy management schemes is validated by means of simulations, under various operating conditions. The results confirm that the implemented scheme has successfully maintained stable common DC bus voltage, ensured continuous bi-directional power supply, and achieved power balance across various operational modes.



Moreover, the ability to maintain the charging levels (SOC) of the battery and supercapacitor within their specified thresholds illustrates efficient energy management and control.

Keywords: Renewable energy sources, photovoltaic (PV) systems, State of Charge, super capacitor,

INTRODUCTION

The growing demand for electricity has led to an increased use of fossil fuels, which in turn has resulted in rising environmental pollution due to the emission of harmful gases such as CO₂ (Carbon Dioxide), CO (Carbon Monoxide), and CH₄ (Methane), etc. To address these challenges, we are turning to renewable energy sources like solar, wind, biomass, hydro, and tidal power, as they are abundantly available in nature. The main problem in using Renewable Energy sources is that they are intermittent. Therefore we are embracing energy storage solutions such as batteries, super capacitors, etc., to capture surplus energy during daylight hours, supplying it to the load, and subsequently releasing stored energy during night time when solar energy isn't available, ensuring continuous power supply. Numerous strategies exist for managing energy and power in grid-connected photovoltaic (PV) systems, each with its own set of benefits and drawbacks [1-3]. Various power management strategies are employed in microgrids to regulate energy distribution and usage, each presenting distinct advantages and disadvantages. An extensive system for control and power management is specifically designed for PV-integrated hybrid microgrid setups, integrating both Alternating Current and Direct Current power lines to support both grid-tied and standalone operational modes. However, power quality issues present certain limitations [4]. A strategy is deployed to regulate the voltage and energy levels of the distribution system in both grid-connected DC Micro grid and islanded DC Microgrid configurations, utilizing hybrid energy storage devices but controlling across multiple micro grids presents challenges [5]. Utilizing battery and supercapacitor (SC) systems to address the demand-generation gap and ensure stability in DC bus voltage is presented [6]. The challenge lies in effectively regulating the currents of both batteries and supercapacitors to meet varying power demands. An energy management strategy is executed for photovoltaic (PV) systems integrated with battery storage within an isolated microgrid setting [7] but the fixed droop slope leads to inadequate distribution of power among sources. The control scheme is designed to synchronize the operating point of the photovoltaic (PV) system with the load whenever the accessible PV power surpasses the load requirement and the battery is fully charged. An enhanced Predictive Power and Voltage Control (MPPVC) model is implemented for the AC/DC interconnected converter, guaranteeing superior voltage quality and facilitating seamless power transfer between AC and DC sub grids[8] by achieving seamless grid synchronization and connection becomes feasible. Subsequently, a comprehensive Energy Management Strategy (EMS) at the system



level is devised to ensure stable operation amidst varying power generation and consumption scenarios. But, challenge arises in stabilizing the DC bus voltage. The Power Management Strategy (PMS) for grid-connected PV systems with a hybrid energy storage system, as presented in [9], effectively manages challenging scenarios for instance, load reduction, and PV operation away from maximum power point., mitigation of hazardous power oscillations in the hybrid energy storage system (HESS), islanded operation, and grid resynchronization. However, it encounters higher levels of harmonic distortion as a limitation. An array of Power Management Strategies has been deployed [10-17], Many effective approaches are presented to ensure precise allocation of load current oscillations and DC components among distributed generation (DG) units within DC Micro grids [18-27]. Yet they encounter certain constraints as the destabilization of systems by partial shading, fluctuating environment conditions, power quality concerns, battery strain from current loads and the need for DC Bus Voltage Regulation also they will no offer cost-effective solutions.

This paper introduces an energy optimization approach developed for a grid-connected system utilizing hybrid energy storage devices, specifically a battery and a supercapacitor. The designed system functions reliably regardless of charging or discharging states, achieving satisfactory state-of-charge (SOC) balancing.

RESEARCH OBJECTIVE:

The primary goals of the proposed energy management scheme are to promptly regulate voltage under uncertain conditions and to rigorously maintain power quality standards. Ensuring that the charging levels (SOC) of both the battery and supercapacitor stays within prescribed threshold values. Monitor the frequency and voltage levels across the entire system to ensure compliance with set thresholds. Monitoring the battery's power supply or absorption, considering the available stored energy, and reducing current stress on the battery. Efficient power flow management between load and generation stringent maintenance of power quality standards.

System Design and Energy Management Strategy: The architecture for grid-interconnected PV is presented in the figure 1. , where L, D, S, C are the inductor, diode, switch, and capacitor of the Boost Converter respectively. V_{BAT} , V_{SC} , V_{DC} , V_{GRID} are the voltages of the battery, supercapacitor, common DC link voltage, and Grid voltage respectively. C_{BAT} and C_{db} are the capacitors for the battery and the bi-directional converter connected to the battery, respectively. C_{SC} , L_F , R_F are the supercapacitor capacitance, inductance and resistance of the low-pass filter respectively. V_{PV} , S_1 , S_2 , S_3 and S_4 are the open-circuit voltage of the PV and IGBT (Insulated Gate Bi-polar Transistor) switches of the Micro grid Converter. S_{b1} , S_{b2} , S_{s1} , S_{s2} are switches of the battery and super capacitor bi-directional converter respectively. R_{NL} , L_{NL} are the resistor and inductor of the non-linear load respectively. R_{LAC} and R_{LDC} are the AC and DC linear loads respectively. L_B , R_B , and



L_{SC} represent the inductor, resistor connected to the battery bi-directional converter, and the inductor of the supercapacitor bi-directional converter, respectively.

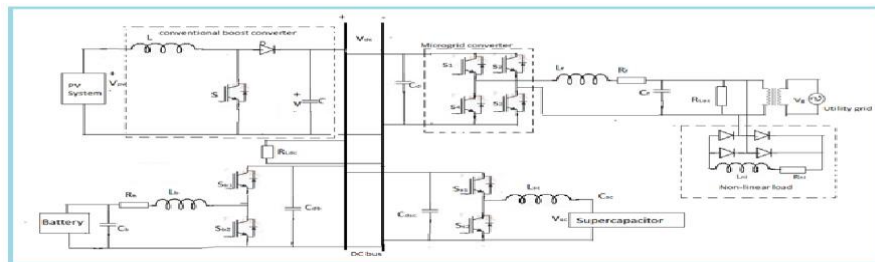


Figure.1 System Architecture of Grid Integrated PV with HEDS

To get a stable common DC-link voltage, the output of the PV should be high but we know that the output of the PV is low, so we use a boost converter to step up the voltage to integrate it with the grid. For energy storage, both the battery and supercapacitor are employed, along with a bi-directional DC-DC Boost converter (BDDC) to regulate power transfer between the grid and the Hybrid Energy Storage Devices (HEDS). The AC Grid is linked to the DC Microgrid through a Voltage Source Converter (VSC), which functions as either an inverter or rectifier depending on the operational mode. The low-pass filter is used at the output of the microgrid converter to smoothen the voltages and currents at the AC side. In this scheme, linear and non-linear loads are connected to the system under different operating modes. This power management strategy primarily involves generating reference current, executing a power management algorithm, and regulating various current converters. The suggested power management arrangement is shown in the below figure 2.

To maintain the stability of the voltage across the Common DC link and to balance power, it is segmented as 3 parts: the mean Power element (P_{avg}), it fluctuates according to changes in PV power based on load requirements; the Transient Power Component (P_{trans}), primarily caused by abrupt fluctuations in PV power and load; and the Oscillatory Power Component (P_{osc}), mainly due to fluctuations in AC power.

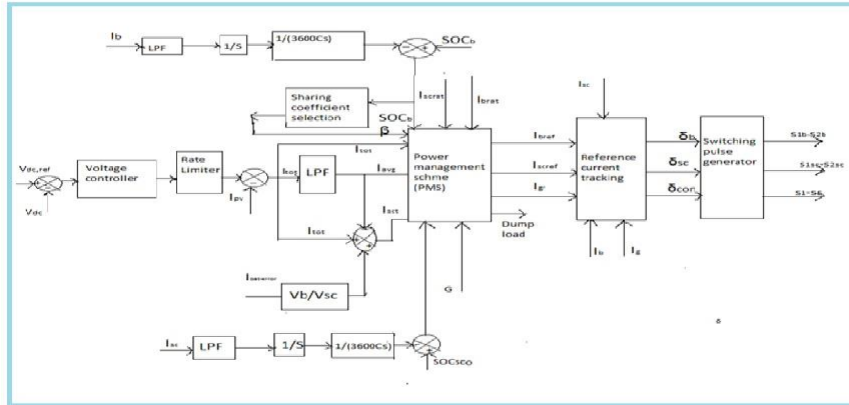


Figure 2: Implemented Power Management Strategy for Grid-Connected PV with HESS Reference Current Generation

By leveraging these power parts, the equilibrium of power available at the common DC link voltage for grid-interconnected Hybrid Energy Storage Devices (HESD) is expressed in the following equation.

$$P_{total}(t) = P_{pv}(t) + P_{bat}(t) + P_{sc}(t) + P_{grid}(t) = P_{avg} + P_{trans} + P_{osc} \quad (1)$$

$$= P_{DCload}(t) + P_{ACload}(t) = P_{load}(t) \quad (2)$$

Referring to equation (1) above, the total Power required to control the voltage of the common DC link (V_{dc}) is expressed as follows.

$$P_{total}(t) = P_{avg} + P_{trans} + P_{osc} = V_{dc} i_{avg} \quad (3)$$

The currents with respect to the above three power components as follows

$$I_{total} = \frac{P_{avg}}{V_{dc}} + \frac{P_{trans}}{V_{dc}} + \frac{P_{osc}}{V_{dc}} = i_{avg} + i_{trans} + i_{osc} \quad (4)$$

The average current (i_{avg}) across the common DC link is determined by the voltage control loop, expressed as follows:

$$I_{total}(t) = K_{Pvol} * V_{dcerror} + K_{Ivol} \int V_{dcerror} dt \quad (5)$$

Separating the three current components at the DC link is essential to enhance the overall system performance. The mean part (i_{avg}) of the overall current is calculated as follows:

$$I_{avg}(t) = I_{total}(t) * \left(1 - \frac{1}{1 + sT_c}\right) \quad (6)$$

The transient component (i_{trans}) of the total current is derived as follows



$$I_{trans}(t) = I_{total}(t) * \left(1 - \frac{1}{1 + sT_c}\right)$$

(7)

The oscillatory component (i_{osc}) of the total current is derived as follows

$$I_{osc}(t) = I_{total}(t) * \left(1 - \frac{1}{1 + sT_c}\right)$$

(8)

The mean part of the overall current is allocated among PV, HEDS, and the Utility Grid. Meanwhile, the transient and oscillatory parts of the overall current are supported by the supercapacitor.

Power Management Scheme (PMS)

The implemented PMS selects the system's operational mode based on the produced PV power and the load requirement. The Power Management Algorithm (PMA) transitions to a voltage-controlled mode when the voltage source converter (VSC) operates independently and shifts to a current-controlled mode when the voltage source converter is connected to the Grid. During islanded conditions, voltage control at the point of common coupling (PCC) is managed by the voltage source converter (VSC) to ensure uninterrupted power supply to the AC load. The three modes mentioned above are determined by the average current (I_{avg}) component. In Deficient Power Mode (DPM) ($P_s > 0$), the power demand from the load exceeds the power generated by the PV system. Therefore, to meet the load demand, power is sourced from the hybrid energy sources until they reach their lower limits, supplemented by the grid when available (i.e., under Grid-on Mode). In Grid-on Mode, if the battery's State of Charge (SOC) falls below the acceptable threshold, the grid will provide power to charge the battery and meet the required load. During Grid-off Mode, the battery supplies the deficient power while adhering to its State of Charge (SOC) limits. If the State of Charge (SOC) falls below the acceptable limit, a portion of the load is shed to ensure power balance is maintained. The range of power sharing coefficient i.e., β for the battery and supercapacitor depending on their SOC limits for all modes is shown below table 1 and table 2 as follows.

Table 1. SOC Values for the Battery

Stage	SOC _{Bat} (t)	β	1 - β
Stage - 1	SOC _B < L	0	1
Stage - 2	0.1 < SOC < 0.3	0.25	0.75
Stage - 3	0.3 < SOC _B < 0.5	0.5	0.5
Stage - 4	0.5 < SOC _B < 0.7	0.7	0.3
Stage - 5	0.7 < SOC _B < U	1	0



Table 2. SOC Values for the Super capacitor

Stage	SOC _{Bat} (t)	β	$1 - \beta$
Stage - 1	SOC _{SC} < L	0	1
Stage - 2	0.1 < SOC _{SC} < 0.3	0.25	0.75
Stage - 3	0.3 < SOC _{SC} < 0.5	0.5	0.5
Stage - 4	0.5 < SOC _{SC} < 0.7	0.7	0.3
Stage - 5	0.7 < SOC _{SC} < U	1	0

The reference current generation and power management in DPM is shown in Table 3 and Table 4.

Table 3. Operational Design in DPM

SOC Range	Reference Current Generation
SOC _B > L and SOC _{SC} > L	$i_{B,r} = \beta i_{avg}$, $i_{SC,r} = i_{tr} + i_{osc}$, $i_{G,r} = (1-\beta)i_{avg}$
SOC _B < L and SOC _{SC} > L	$i_{B,r} \cong 0$, $i_{SC,r} = i_{tr} + i_{osc}$, $i_{G,r} = i_{avg}$
SOC _B > L and SOC _{SC} < L	$i_{B,r} = \beta i_{avg}$, $i_{SC,r} \cong 0$, $i_{G,r} = (1-\beta)i_{avg}$
SOC _B < L and SOC _{SC} < L	$i_{B,r} \cong 0$, $i_{SC,r} \cong 0$, $i_{G,r} = i_{avg}$

Table 4. Power Generation in DPM

SOC Range	Reference Power
SOC _B > L and SOC _{SC} > L	$P_{B,r} = \beta P_{avg}$, $P_{SC,r} = P_{tr} + P_{osc}$, $P_{G,r} = (1-\beta)P_{avg} + P_{loss}$
SOC _B < L and SOC _{SC} > L	$P_{B,r} \cong 0$, $P_{SC,r} = P_{tr} + P_{osc}$, $P_{G,r} = P_{avg} + P_{loss}$
SOC _B > L and SOC _{SC} < L	$P_{B,r} = \beta P_{avg}$, $P_{SC,r} \cong 0$, $P_{G,r} = (1-\beta)P_{avg} + P_{loss}$
SOC _B < L and SOC _{SC} < L	$P_{B,r} \cong 0$, $P_{SC,r} \cong 0$, $P_{G,r} = P_{avg} + P_{loss}$

Converter Control for HEDS

The control of the Battery converter consists of the reference current generation ($i_{BAT_ref}^*$), rate limiter function (f_{RTL}), Power Management Algorithm (PMA), and the average power-sharing constant (or) distribution factor (β) selection depending on the SOC of the battery. The reference current for the battery, which is connected to the bi-directional converter, is expressed as follows:

$$i_{BAT_ref}^*(t) = f_{BAT}(PMA) \lambda \left(\frac{1}{T} \int_{t_0 - T_{BAT}}^{t_0} i_{avg}(t) dt \right) f_{RTL}(t) \quad (9)$$

The controlling signal (δ_{BAT}) of the battery bidirectional converter is expressed as shown below.

$$\delta_{BAT} = K_{P,BAT} i_{BAT} + e(t) +$$



$$\frac{K_{iBAT}}{T_{BAT}} \int_{t-T_{BAT}}^t i_{BAT}, e(t) dt \quad (10)$$

The control of the Supercapacitor converter comprises the generation of reference current (i_{SC_ref}), the rate limiter function (fRTL), and the Power Management Algorithm (PMA). The expression for the reference current and controlling signal of the supercapacitor bidirectional converter is shown below.

$$i_{SC,ref}(t) = i_{total}(t) - \frac{1}{T_{SC}} \int_{t_0-T_{SC}}^{t_0} i_{total}(t) dt + G' (V_{dcr} - V_{dc}) \quad (11)$$

Where, $G' = \frac{V_{BAT}}{V_{SC}}$ (12)

$$\delta_{SC} = K_{P,SC} * i_{SC}, e(t) + \frac{K_{iSC}}{T_{SC}} \int_{t-T_{SC}}^t i_{SC}, e(t) dt \quad (13)$$

Converter Control for PV

The reference current for the PV converter is selected to facilitate the operation of the system across all three power modes. The selected PV reference current (i_{PV_ref}) is subsequently compared with the actual current of the boost converter and regulated using the PI (Proportional Integral) current controller. The reference current for PV is generated by the Power Management Algorithm (PMA). The control or modulation signal for the PV Converter is as follows.

$$\delta_{PV_A} = K_{Pro,PV} * i_{PV}, e(t) + \frac{K_{iPV}}{T_{PV}} \int_{t-T_{PV}}^t i_{PV}, e(t) dt \quad (14)$$

Converter Control for VSC (Voltage Source Converter)

The VSC control primarily includes reference current generation, voltage template computation, and current control. Depending on the PV Power generated, the VSC acts as an inverter (or) generator. The reference current for the VSC is generated depending on the bidirectional power flow from the AC grid to the DC link or vice versa. The reference current for the VSC is determined as follows.

$$i_{GRID_ref} = \begin{cases} (1-\beta) i_{avg}(t) * f_{CTRL}(t) \sin \omega t & \text{if } P_S > 0 \text{ (DPM)} \\ i_{avg}(t) \sin \omega t & \text{if } P_H < 0 \text{ (EPM)} \end{cases} \quad (15)$$

(16)

The below figure (6) shows the overall control structure for PV, Battery, supercapacitor and VSC control as follows.

SIMULATION RESULTS

The proposed energy management scheme's performance analysis is rigorously validated through extensive simulation work using MATLAB/Simulink software, encompassing various loading conditions. The parameters of the system for simulation studies are outlined in the following Table 6



Table 6. System Parameters

SYSTEM PARAMETERS	
Supercapacitor Pack Parameters	Values
Terminal Voltage (V_{SC})	200V
Max. Peak Current (I_P)	500A
Capacitance/Pack (C_{SC})	3F
Max. Continuous Current (I_{MC})	10A
Battery Pack Specifications	Values
Ah Capacity	100Ah
Terminal Voltage (V_B)	200V
No. Of Batteries in series	66
Battery Converter Parameters	$L_b = 1\text{mH}$, $C_b = 100\mu\text{F}$
Supercapacitor Converter Parameters	$L_{SC} = 1\text{mH}$
VSC Parameters	$L_f = 0.1\text{mH}$, $C_f = 10\mu\text{F}$, $C_{di} = 12000\mu\text{F}$
Boost Converter Parameters	$L_1 = 1\text{mH}$, $C_1 = 100\mu\text{F}$
Parameters of PI Controller's	Values
Supercapacitor	$K_{P, SC} = 0.001$, $K_{i, SC} = 0.000025$
Battery	$K_{P, BAT} = 0.001$, $K_{i, BAT} = 0.000025$
PV	$K_{P, PV} = 0.001$, $K_{i, PV} = 0.000025$
DC link Voltage	$K_{P, DC} = 0.01$, $K_{i, DC} = 0.005$
AC and DC Load Parameters	$R_{Lac} = 20\Omega$, $R_{Ldc} = 20\Omega$
Utility and DC Link Parameters	$V_g = 230\text{V}$, $f = 50\text{HZ}$, $V_{dc} = 400$

The performance of the system is assessed under both Discrete Power Mode (DPM) and Embedded Power Mode (EPM) scenarios, across various operational modes, depending on the state of charge of energy storage devices and load conditions.

Performance with DPM:

The PV specifications are detailed as follows: 10 parallel strings, each with 5 series-connected modules per string, containing 80 cells per module, with a maximum power output of 334.905 W. Throughout the time span of 1-5 seconds, the PV current fluctuates in response to varying irradiances. Notably, despite these changes in irradiance, the PV voltage remains nearly constant.

The system comprises both an AC load rated at 8 kW and a DC load also rated at 8 kW. The irradiation levels vary dynamically, starting at 300 W/m² and transitioning to 500 W/m² from 1.5 seconds to 2.5 seconds, followed by a decrease to 150 W/m² from 2.5 seconds to 3 seconds. Subsequently, the irradiation rises to 600 W/m² from 3 seconds to 4.5 seconds, and



then decreases to 450 W/m² from 4.5 seconds to 5 seconds. Figure 5 depicts the total power distribution among the PV system, battery, super capacitor, AC load, grid, and inverter.

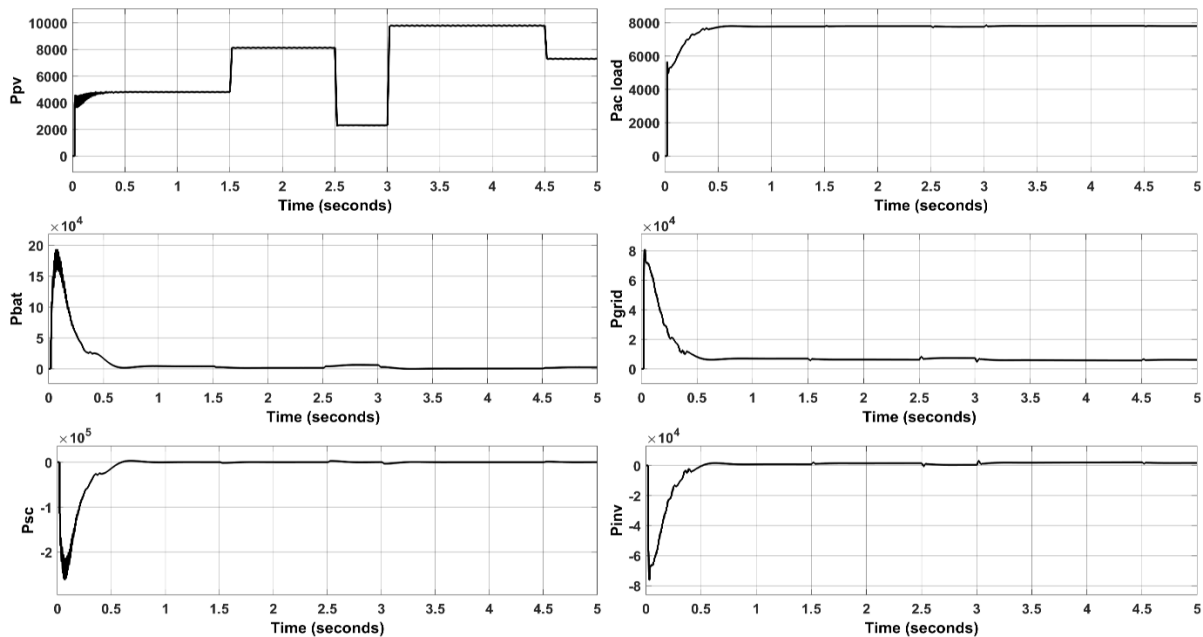


Fig. 5. Powers of PV, Battery, Supercapacitor, AC Load, Grid and Inverter

According to the plot above, the PV power generation initiates at 4200 W, escalates to 8000 W at 1.5 seconds, aligned with an irradiation level of 500 W/m². Subsequently, it decreases to 2200 W at 2.5 seconds, corresponding to an irradiation of 150 W/m². At 3 seconds, the PV power peaks at 9400 W, correlating with an irradiation of 600 W/m², and then stabilizes at 7200 W at 4.5 seconds, coinciding

with an irradiation of 450 W/m². As evident from the data, the grid power remains constant at 0.8 kW. This is due to the system operating under DPM, where the grid is precisely supplying the necessary load power equivalent to 8 kW.

In deficit power mode, the battery functions to provide any shortfall in power, taking into account its state of charge (SOC) and predefined boundaries taken as 80% and 50% respectively. The battery and supercapacitor undergo four distinct states, encompassing both charging and discharging phases.

PV power and load demand corresponding to state -1 operation are summarized in the tables shown below where CGR stands for charging, DCGR for discharging, SHRL for sharing the load, and for receiving power.



Table 7. The functionality of the proposed energy management scheme in response to fluctuations in both PV output and load power with DPM..

Mode	DPM(Deficit Power Mode)				
	T ₁ =0.5	T ₂ =1.5	T ₃ =2.5	T ₄ =3	T ₅ =4.5
Time Instants(sec)	T ₁ =0.5	T ₂ =1.5	T ₃ =2.5	T ₄ =3	T ₅ =4.5
SOC _{BAT}	>LL	>LL	>LL	>LL	>LL
SOC _{SC}	>LL	>LL	>LL	>LL	>LL
Battery mode	DCGR	DCGR	DCGR	DCGR	DCGR
Supercapacitor mode	DCGR	DCGR	DCGR	DCGR	DCGR
Utility Grid mode	SHRL	SHRL	SHRL	SHRL	SHRL
Irradiations (W/M ²)	300	500	150	600	450
AC Load Power (W)	7798	7798	7798	7798	7798
DC Load Power (W)	7798	7798	7798	7798	7798
Accumulated PV power(W)	4500	8100	2200	9700	7312
Grid Power(W)	8000	7000	8500	6500	6170
Battery power(W)	3000	2000	6000	1200	2519
Supercapacitor power(W)	-300	-900	900	-900	-13.45

According to the table above, during Deficit Power Mode (DPM), at the moment T₁=1.5 sec, The battery and utility grid together supply the power needed to meet the deficient load. Based on the state of charge (SOC) conditions of the energy storage devices, the system dynamically transits between different modes according to PV power availability and load demands. The supercapacitor packs handle transient power surges resulting from abrupt changes in PV output and load. Any surplus mean power associated with the DC link is utilized either to refill the battery, contingent upon the charging levels (SOC) of the battery and supercapacitor, or injected into the grid.

CONCLUSION

A dynamic Energy Management strategy is deployed in a grid-tied PV system with hybrid energy storage devices. It has been demonstrated that the implemented scheme ensures stable common DC bus voltage, achieves continuous bi-directional power supply, and maintains power balance across different modes by keeping the charging (SOCs) of the battery and supercapacitor within their threshold values. The results suggest that employing a high-power-density supercapacitor pack efficiently regulates the DC link voltage, thus alleviating strain on the battery. Hence, this suggested hybrid energy management strategy can also prolong the lifespan pertaining to the battery. Compared to other schemes the performance of



the system is better and THD is reduced i.e., 1.11%, thus improving the power quality.

REFERENCES

1. S. K. Kollimalla and M. K. Mishra, "A novel adaptive P&O MPPT algorithm considering sudden changes in the irradiance," *IEEE Transactions on Energy Conversion*, vol. 29, no. 3, pp. 602-610, May 2014.
2. S. Mishra and R. K. Sharma, "Dynamic power management of PV based islanded microgrid using hybrid energy storage," in *Proceedings of IEEE 6th International Conference on Power Systems (ICPS)*, New Delhi, India, Mar. 2016, pp. 1-6.
3. C. Natesan, S. Ajithan, S. Chozhavendhan *et al.*, "Power management strategies in microgrid: a survey," *International Journal of Renewable Energy Research*, vol. 5, no. 2, pp. 334-340, Jan. 2015.
4. Z. Yi, W. Dong, and A. H. Etemadi, "A unified control and power management scheme for PV-battery-based hybrid microgrids for both grid-connected and islanded modes," *IEEE Transactions on Smart Grid*, vol. 9, no. 6, pp. 5975-5985, Nov. 2018.
5. S. Pannala, N. Patari, A. K. Srivastava *et al.*, "Effective control and management scheme for isolated and grid-connected DC microgrid," *IEEE Transactions on Industry Applications*, vol. 56, no. 6, pp. 1-14, Dec. 2020.
6. P. Singh and J. S. Lather, "Variable structure control for dynamic power-sharing and voltage regulation of DC microgrid with a hybrid energy storage system," *International Transaction Electrical Energy System*, vol. 30, no. 9, pp. 1-20, Jun. 2020.
7. H. Mahmood, D. Michaelson, and J. Jiang, "A power management strategy for PV/battery hybrid systems in islanded microgrids," *IEEE Journal of Emerging and Selected Topics in PowerElectronics*, vol. 2, no. 4, pp. 870-882, Jun. 2014.
8. J. Hu, Y. Shan, Y. Xu *et al.*, "A coordinated control of hybrid AC/DC microgrids with PV-wind-battery under variable generation and load conditions," *Electrical Power and Energy Systems*, vol. 104, pp. 583- 592, Jan. 2019.
9. H. Wang, Z. Wu, G. Shi *et al.*, "SOC balancing method for hybrid energy storage system in microgrid," in *Proceedings of 3rd IEEE International Conference on Green Energy and Applications*, Taiyuan, China, Oct. 2019, pp. 141-145.
10. P. Sanjeev, N. P. Padhy, and P. Agarwal, "Peak energy management using renewable integrated DC microgrid," *IEEE Transactions on Smart Grid*, vol. 9, no. 5, pp. 4906-4917, Sept. 2018.
11. S. Sahoo, S. Mishra, and N. P. Padhy, "A decentralized adaptive droop-based power management scheme in autonomous DC microgrid," in *Proceedings of IEEE PES Asia-Pacific Power and Energy Conference*, Xi'an, China, Dec. 2016, pp. 1018-1022.



12. P. Singh and J. S. Lather, "Power management and control of a grid independent DC microgrid with hybrid energy storage system," *Sustainable Energy Technologies and Assessments*, vol. 43, pp. 1-11, Feb. 2021.
13. R. Kadri, J. P. Gaubert, G. Champenois *et al.*, "Performance analysis of transformerless single switch quadratic boost converter for grid-connected photovoltaic systems," in *Proceedings of International Conference on Electrical Machines (ICEM)*, Rome, Italy, Sept. 2010, pp. 1-7.
14. M. Hamzeh, A. Ghazanfari, Y. A. R. I. Mohamed *et al.*, "Modelling and design of an oscillatory current sharing control strategy in DC microgrids," *IEEE Transactions on Industrial Electronics*, vol. 62, no. 11, pp. 6647-6657, Nov. 2015.
15. B. Singh, D. T. Shahani, and A. K. Verma, "IRPT based control of a 50 kW grid interfaced solar photovoltaic power generating system with power quality improvement," in *Proceedings of 4th IEEE International Symposium on Power Electronics for Distributed Generation System (PEDG)*, Rogers, USA, Apr. 2014, pp. 1-8.
16. S. Golestan, M. Ramezani, J. Guerrero *et al.*, "Moving average filterbased phase-locked loops: performance analysis and design guidelines," *IEEE Transactions on Power Electronics*, vol. 29, no. 6, pp. 2750-2763, Jun. 2014.
17. N. R. Tummuru, M. K. Mishra, and S. Srinivas, "Dynamic energy management of renewable grid integrated hybrid energy storage system," *IEEE Transactions on Industrial Electronics*, vol. 62, no. 12, pp. 7728-7737, Dec. 2015.
18. H. Wang, Z. Wu, G. Shi *et al.*, "SOC balancing method for hybrid energy storage system in microgrid," in *Proceedings of 3rd IEEE International Conference on Green Energy and Applications*, Taiyuan, China, Oct. 2019, pp. 141-145.
19. S. Kotra and M. K. Mishra, "A supervisory power management system for a hybrid microgrid with HESS," *IEEE Transactions on Industrial Electronics*, vol. 64, no. 5, pp. 3640-3649, May 2017.
20. Bogimi Sirisha, Saieni Akhilesh, "High efficient and high gain boost converter with soft switching capability connected to grid using dq axis current control", *Bulletin of Electrical Engineering and Informatics*, Vol. 11, No. 2, April 2022, pp. 624~635 ISSN: 2302-9285, DOI: 10.11591/eei.v11i2.3358.
21. Bogimi Sirisha, Laxminarayana Yalakanti, "A mitigation technique for torque ripple in a brushless DC motor by controlled switching of small DC link capacitor", *Bulletin of Electrical Engineering and Informatics*, Vol. 11, No. 2, April 2022, pp. 624~635 ISSN: 2302-9285, DOI: 10.11591/eei.v11i2.3408.
22. B.Sirisha, Nazeemuddin, "A Novel Five-Level Voltage Source Inverter interconnected to Grid with SRFCcontroller for voltage synchronization" , *Bulletin of Electrical Engineering and Informatics*, Vol. 11, No.1,February 2022, ISSN: 2302-9285, DOI:



10.11591/eei.v11i1.3274.

23. B. Sirisha "A grid interconnected nested neutral point clamped inverter with voltage synchronization using synchronous reference frame controller", International Journal of Applied Power Engineering (IJAPE) , Vol. 10, No. 4, December 2021, pp. 364~372 ISSN: 2252-8792, DOI: 10.11591/ijape.v10.i4.
24. Sirisha Bogimi , Manorama Vattoli, "Design of High gain Boost Converter for Standalone applications", Gradiva Review Journal, Volume 8, Issue 2 , 2022, pp 270-280, ISSN NO : 0363-8057.
25. B. Sirisha, Sai Mahesh Kurre, J. Upendar, "Design And Analysis Of A Dc-Dc Boost Converter With Solar PV Module Integrated To Three- Phase Grid Using SRF Controller", Journal of Emerging Technologies and Innovative Research(JETIR), Vol 9, Issue 1, Jan-2022, pp. b551-b555, ISSN: 2349-5162.
26. Jalla Upendar, Sangem Ravi Kumar, Sapavath Sreenu, Bogimi Sirisha, "Implementation and study of fuzzy based KY boost converter for electric vehicle charging", International Journal of Applied Power Engineering (IJAPE) Vol. 11, No. 1, March 2022, pp. 91~103 ISSN: 2252-8792, DOI: 10.11591/ijape.v11i1.
27. Sapavath Sreenu, Jalla Upendar, Bogimi Sirisha, "Analysis of switched impedance source/quasi-impedance source DC-DC converters for photovoltaic system", International Journal of Applied Power Engineering (IJAPE) Vol. 11, No. 1, March 2022, pp. 14-24, ISSN: 2252-8792, DOI: 10.11591/ijape.v11i1.